A tunable stiffness diamagnetic levitation accelerometer with flexible sensing performance

Yuanping XU*, Yang WANG*, Jarir MAHFOUD**, and Jin ZHOU*
*College of Mechanical and Electrical Engineering, Nanjing University of Aeronautics and Astronautics
29 Yudao Street, 210016, Nanjing, China
E-mail: ypxu@nuaa.edu.cn
**INSA-Lyon, CNRS UMR5259, LaMCoS
F-69621 Villeurbanne Cedex, France

Abstract
Although diamagnetic levitation technology holds great promise for the development of high-sensitivity accelerometers, the existing designs typically rely on fixed stiffness structures, which significantly limit their adaptability to diverse environmental and measurement conditions. In this work, we propose a feasible static magnetic field control strategy to dynamic modulate the stiffness of diamagnetic levitation accelerometer. A quasi-zero stiffness (QZS) diamagnetic structure is first established, followed by the integration of additional Helmholtz coils to manipulate the external static magnetic field. This enables precise tuning of the potential well distribution of sensitive element. Theoretical analysis demonstrates that this tunable potential approach allows effective control of magnetic stiffness over a wide range from 3.0×10^{-4} to 2.8×10^{-2} N/m. As a result, the accelerometer exhibits flexible sensing performance, yielding ultra-high sensitivity up to 2068 mm/g and an ultra-wide detection range spanning from ±0.30 mg to ±62.7 mg.

Keywords : Diamagnetic levitation, Accelerometer, Tunable stiffness, Static magnetic field, Quasi zero stiffness.

1. Introduction

Diamagnetic levitation refers to the phenomenon that diamagnetic materials generate a repulsive force to counteract gravity in the presence of an external magnetic field (Geim et al., 1999, Berry et al., 1997, Ikezoe et al., 2002, Gao et al., 2019a, Ge et al., 2020 and Nakashima et al.,2020). Diamagnetic levitation technology possesses the key benefits including low power consumption, cost efficiency and reduced mechanical stiffness, making it well-suited for constructing precision sensors, where minimal mechanical contact is crucial (Abadie et al., 2011, Pinot et al., 2017, Gao et al., 2019b).

Up to date, quite a few diamagnetic levitation sensors with capability in detecting forces or density have been reported (Gao et al., 2019b, Zhang et al., 2018, Vikrant and Jayanth, 2022, Yin et al., 2022, Leng et al.,2021). Particularly, the accelerometers based on diamagnetic levitation have gained special attention due to the reported high sensitivity to minute changes in acceleration, enabling precise measurements in a wide range of applications. One of the earliest diamagnetic levitation accelerometers can be traced to the work conducted by Chen et al. (2021, 2022, 2020). They reported a diamagnetic levitation accelerometer consisting of square pyrolytic graphite sheet (sensitive element) and "Opposite 2D" magnet array. The obtained stiffness was 1.47×10^{-1} N/m, yielding theoretical high precision of 0.16 ng/Hz$^{0.5}$ (Chen et al., 2021, Chen et al., 2022 and Chen et al., 2020). Then, Wang developed a diamagnetic levitation accelerometer compromising suspended magnet (sensitive element), lifting magnet array and pyrolytic graphite stator, attaining low stiffness and high precision of 8.1×10^{-3} N/m and 20 ng/Hz$^{0.5}$, respectively (Wang et al., 2020). On the basis of Wang's work, Du employed high-precision laser displacement detection technology to further enhance the precision of accelerometer (<15 ng/Hz$^{0.5}$) (Leng et al., 2024).

Despite the significant and ongoing advancements in diamagnetic levitation accelerometers, it is important to highlight that the current designs still rely on a fixed stiffness structure. To achieve high sensitivity, efforts have been made to reduce the stiffness via optimizing magnetic field properties of permanent magnets or modifying the morphology and mass of sensitive element. While further refining topological structure of sensitive element can direct stiffness

towards "near-zero" levels, this often comes at the cost of dramatically declined detection range. In this context, the dependence on a fixed stiffness structure limits the adaptability of accelerometer, hindering its ability to adjust performance to accommodate varying environmental conditions, such as fluctuations in vibrations or external disturbances. Additionally, specific measurement requirements that demand tailored stiffness characteristics for optimal performance cannot be achieved with a fixed stiffness design (Hussein et al., 2024, Middlemiss et al., 2017). While a fixed stiffness structure offers stability and accuracy in controlled environments, it compromises the versatility and overall performance of accelerometer in dynamic or highly variable settings. This limitation highlights the need for more flexible design approaches to enhance both adaptability and performance in diverse practical applications.

Herein, we present a novel diamagnetic levitation accelerometer with tunable stiffness design. For the first time, a static magnetic field control strategy is introduced to achieve dynamic stiffness adjustment. Specifically, a “quasi-zero” stiffness structure of accelerometer is constructed, which consists of a levitating magnet (sensitive element), lifting magnet array, a diamagnetic stator made of pyrolytic graphite. Then, additional Helmholtz coils are introduced to regulate the external static magnetic field, enabling precise control over the magnetic field distribution within the "quasi-zero" stiffness diamagnetic structure. This approach allows for fine-tuned modulation of the spatial distribution of potential well, and consequently, the horizontal magnetic stiffness of the sensitive element.

In this paper, a comprehensive theoretical study is conducted to investigate the working mechanism of static magnetic field in modulating stiffness and sensing performance of diamagnetic levitation accelerometer. Section 2 describes the overall structure of diamagnetic levitation accelerometer and theoretical model. In Section 3, the simulation results demonstrate the feasibility of static magnetic field in effectively adjusting the stiffness of accelerometer over a wide range, underscoring the adaptability and versatility of tunable stiffness structure.

2. Structure and Modeling

2.1 Structure of diamagnetic levitation accelerometer

The schematic of the proposed diamagnetic levitation accelerometer is depicted in Fig. 1. This accelerometer comprises several key components: a levitating magnet (the sensitive element), a lifting magnet array, a pyrolytic graphite stator, Helmholtz coils, and an optical displacement detection probe. The levitating magnet is made of NdFeB (2×2×2 mm, with axial magnetization strength M_s = 7.5×10^5 A/m). The stator is constructed from highly oriented pyrolytic graphite sheets (10×10×3 mm), which possess an axial magnetization susceptibility of $x_m \approx -450\times10^{-6}$.

The lifting magnet array utilizes an axial "Opposite" configuration, consisting of two NdFeB permanent magnets with different sizes and axial magnetization properties: PM1 (8×8×4 mm, magnetization strength M_{s1}' = 9.5×10^5 A/m) and PM2 (4×4×2 mm, magnetization strength M_{s2}' = -9.5×10^5 A/m).

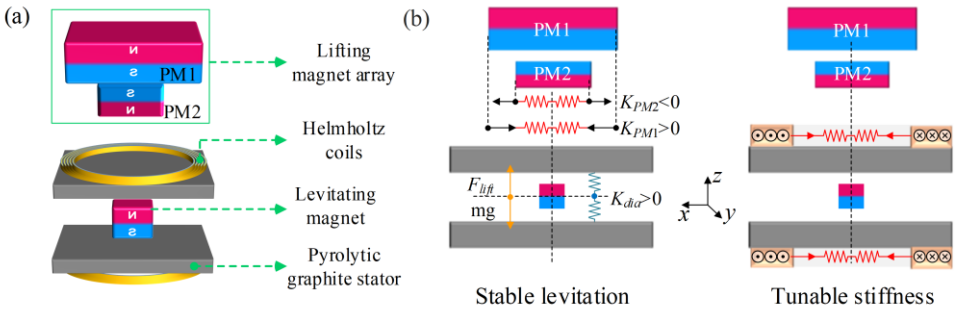

Fig.1 (a) Schematic of the proposed diamagnetic levitation accelerometer, (b) stable levitation and stiffness characteristics of diamagnetic levitation accelerometer.

Due to the interaction between the lifting magnet array and the sensitive element, the latter experiences an upward magnetic force F_{lift} along the vertical (z) axis. This force counteracts the gravitational force mg, achieving a force equilibrium at the levitation point. In addition, the diamagnetic repulsion between the pyrolytic graphite stator and the sensitive element introduces a stabilizing magnetic stiffness K_{dia}>0 along the z-axis, which enables passive self-stabilization of the levitated component, as illustrated in Fig. 1(b).

Crucially, by arranging the magnetic poles of the two lifting magnets in an opposing axial configuration, the system induces both positive and negative magnetic stiffness components along the horizontal (x) axis. These opposing effects result from the magnetic field gradients produced by each magnet. By precisely adjusting the vertical positions (heights, hh) of the two lifting magnets, the positive and negative stiffness components can be finely tuned to cancel each other.

This balancing leads to a near-zero net stiffness—referred to as a "quasi-zero stiffness" characteristic—along the x-axis, which enhances the accelerometer's sensitivity in the measurement direction, as shown in Fig. 1(b).

Based on the "quasi-zero" stiffness configuration, an additional static magnetic field regulation system is introduced, utilizing Helmholtz coils. Specifically, two coils are symmetrically positioned on the upper and lower sides of the sensitive element (see Fig. 1(a)). When equal magnitudes of direct current (DC) are applied to both the upper and lower coils, the generated magnetic field guides the surrounding magnetic flux near the levitation point. This setup effectively alters the spatial magnetic field distribution—modifying both its direction and gradient. As a result, the system enables precise and efficient control over the magnetic stiffness of the sensitive element, as illustrated in Fig. 1(b).

2.2 Working principle

When the diamagnetic levitation accelerometer experiences base vibration, the corresponding base vibration acceleration signal can be obtained by detecting the relative displacement of sensing element along the x measurement axis.

The dynamic equation of sensing element can be simplified into a one-dimensional form that relates to the displacement along *x* measurement axis:

$$m\ddot{x}_r + c\dot{x}_r + K(I)x_r = -ma \tag{1}$$

where m is the mass of sensing element, x_r is the relative displacement between sensing element and stator, a represents the base vibration acceleration, $K(I)$ is the magnetic stiffness of sensing element which can be adjusted by varying static magnetic field, and c is the electromagnetic damping coefficient derived from the eddy current effect.

By applying the Laplace transform to equation (1), we can derive the transfer function (2) that describes the relationship between the input acceleration signal and the output displacement signal.

$$X_r(\omega)/A(\omega) = 1/\omega_n^2 \sqrt{(1-(\omega/\omega_n)^2)^2 + [2\zeta(\omega/\omega_n)]^2} \tag{2}$$

Where $\zeta = c/(m \cdot K(I))^{0.5}$ represents the damping factor, while $\omega_n = (K(I)/m)^{0.5}$ denotes the natural frequency of diamagnetic structure. In principle, by adjusting $K(I)$, ω_n can be modified to alter the relationship between input acceleration and output displacement. Consequently, one can then modulate the sensing performance, i.e., sensitivity of accelerometer.

2.3 Modeling of diamagnetic levitation structure

The magnetic stiffness of a diamagnetic structure is theoretically determined primarily by the distribution of the magnetic potential well, which results from the interaction between the external magnetic field and the sensitive element. To gain a deeper understanding of the effect and underlying mechanism of the external magnetic field on the magnetic stiffness of a diamagnetic structure, a magnetic dipole model is utilized to theoretically describe the magnetic potential energy distribution of the diamagnetic levitation system, as illustrated in Fig. 2.

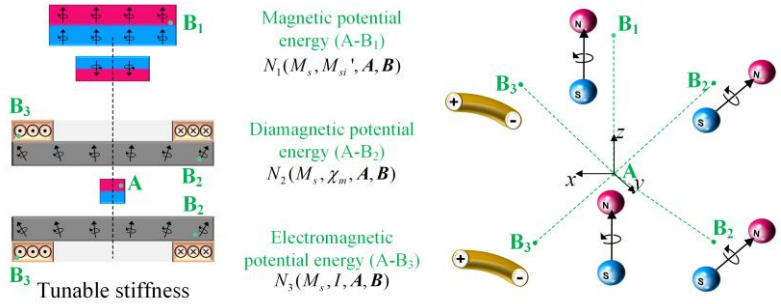

Fig.2 Schematic diagram of the interaction between magnetic dipoles.

According to the principle of virtual work, the levitation state of the sensitive element can be described by its potential energy distribution characteristics. When the potential energy distribution of the sensitive element forms a potential well structure, passive self-stabilized levitation is achieved. In this case, as indicated by equation (3), the sensitive element is in force equilibrium ($\boldsymbol{F}$=0) at the levitation position. Furthermore, it experiences a positive magnetic stiffness, as described in equation (4):

$$\boldsymbol{F} = -\nabla U_{total} = \mathbf{0} \tag{3}$$

$$K_j = -\frac{\partial^2 U_{total}}{\partial^2 x_j} \tag{4}$$

Where F represents external force acting on the sensitive element, U_{total} refers to the total potential energy of sensitive element, x_j (j=1,2,3) represents the displacement of the sensitive element along the x, y, and z axis respectively, and K_j (j=1,2,3) refers to the magnetic stiffness of the sensitive element along the x, y, and z axis respectively.

Then, the U_{total} can be described by Equation(5) which summarizes the potential energy of sensitive element induced by external factors, as follows：

$$U_{total} = \sum_{i=1}^{4} U_i = \sum_{i=1}^{3} \int_{V_M} \int_{V_i} N_i \cdot dv_i \cdot dv_m + \int_{V_M} \rho g z \cdot dv_m \tag{5}$$

Where U_i (i=1,2,3,4) denote the magnetic potential energy induced by lifting magnet array, the magnetic potential energy originated from the interaction with pyrolytic graphite stator, the electromagnetic potential energy generated by Helmholtz coils, and the gravitational potential energy in Earth's gravitational field, respectively; N_i (i=1,2,3) correspond to the magnetic potential energy per unit volume of sensitive element induced by the lifting magnet unit, diamagnetic material unit and current element in the Helmholtz coils, respectively. The expressions for these potential energies are as follows:

$$N_1(M_s, M_{si}', \boldsymbol{A}, \boldsymbol{B}) = -\frac{\mu_0 M_s \cdot M_{si}'}{4\pi}\left[3\frac{(z_a - z_b)^2}{r^5} - \frac{1}{r^3}\right] \tag{6}$$

$$N_2(M_s, \chi_m, \boldsymbol{A}, \boldsymbol{B}) = \frac{\mu_0 \chi_m M_s^{\,2}}{32\pi^2 \mu_r}\left[3\frac{(z_a - z_b)^2}{r^5} - \frac{1}{r^3}\right]^2 \tag{7}$$

$$N_3(M_s, I, \boldsymbol{A}, \boldsymbol{B}) = \frac{\mu_0 M_s \cdot I}{4\pi}\frac{x_a x_b + y_a y_b - x_a^{\,2} - y_a^{\,2}}{r^3\sqrt{x_a^{\,2} + y_a^{\,2}}} \tag{8}$$

Where M_s denote the magnetization strength of sensitive element; M_{si}' represent the magnetization strength of lifting magnet array; x_m is the magnetic susceptibility of pyrolytic graphite stator; I is the current passing through the Helmholtz coil; $\boldsymbol{A}$ represents one observation point on the sensitive element, and $\boldsymbol{B_i}$ (i=1,2,3) refer to the source points located on the lifting magnet array, pyrolytic graphite stator and Helmholtz coil, respectively.

3. Theoretical modeling results

Based on the above analysis, it can be concluded that by adjusting the current passing through the Helmholtz coils, both the magnetic potential energy and stiffness of the diamagnetic levitation structure can be effectively regulated. Fig.4 illustrates the theoretical magnetic potential energy, stiffness and dynamic response of sensitive element (using theoretical model aforementioned) along horizontal measurement axis upon varied applied currents (-85~31 mA). One can see that as the applied current varied from -85 mA to 31 mA, a smoother spatial distribution of potential well reduced stiffness in the horizontal axis (from 2.8×10^{-2} to 3.0×10^{-4} N/m). Concurrently, the decreased magnetic stiffness results in an increased dynamic response of the sensitive element when subjected to vibrations of the same acceleration amplitude (50 ug), as shown in Fig.3 (c).

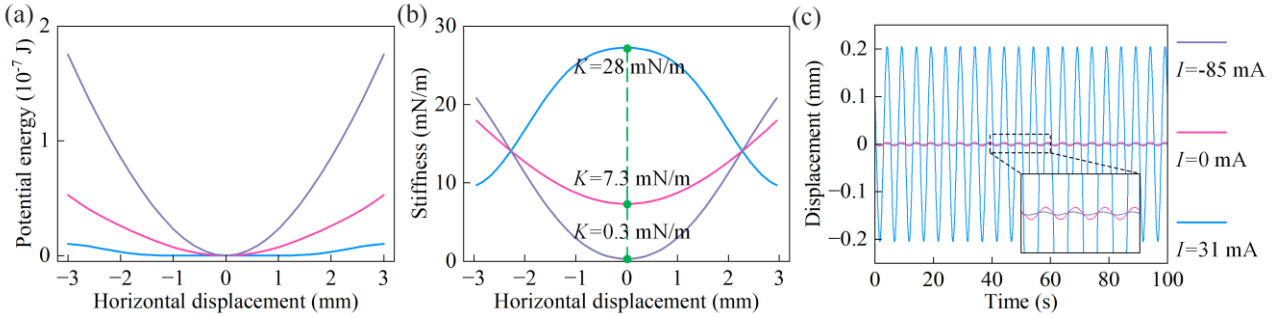

Fig.3 (a) Magnetic potential energy versus displacements, (b) horizontal magnetic stiffness versus displacements and (c) dynamic response upon the 50 ug acceleration vibrations under three representative cases where $I = 0$, $I > 0$ (31 mA) and $I < 0$ (-85 mA).

Then, the natural frequency, sensitivity, and input-output relationship of diamagnetic structure can be derived using equation (2) and the theoretical magnetic stiffness. The obtained results are manifested in Fig.4 (a) and (b), respectively. As the applied current varied from -85 mA to 31 mA, the gradually decreasing theoretical magnetic stiffness would also induce the decreasing natural frequency of measurement axis (from 3.42 Hz to 0.32 Hz). Similarly, with decreasing magnetic stiffness, the detection range also exhibits a downward trend, decreasing from ±62.7 to ±0.30 mg. However, the sensitivity exhibits a upward trend with decreasing magnetic stiffness, increasing from 21.7 to 2068 mm/g.

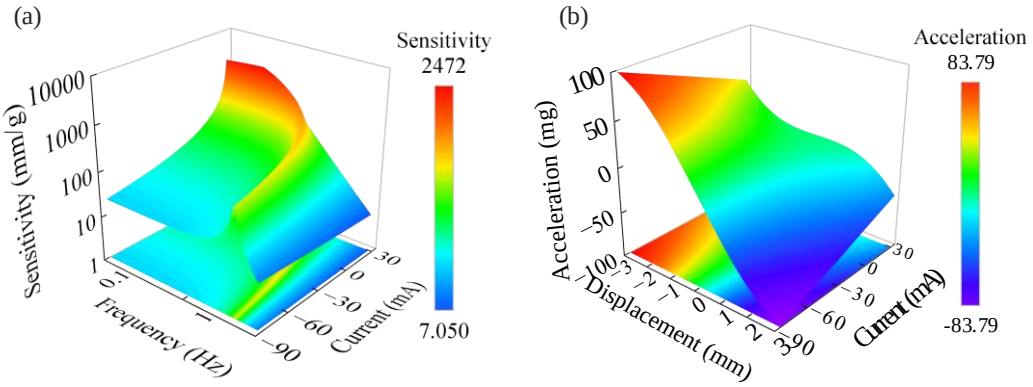

Fig.4 (a) Frequency response curves and (b) input-output relationship of diamagnetic accelerometer versus varied current through Helmholtz coils.

4. Conclusion

This work presents a theorical design of a novel diamagnetic levitation accelerometer with tunable stiffness capability via static magnetic field strategy. Initially, a “quasi-zero” stiffness diamagnetic levitation structure is constructed by strategically arranging the magnetic poles of a lifting magnet array in opposition. Subsequently, Helmholtz coils are employed to regulate the external static magnetic field, thereby controlling the horizontal magnetic stiffness of the sensitive element. A theoretical model of diamagnetic levitation structure is developed to elucidate the influence of the external static magnetic field on the system. The theoretical results demonstrate that the accelerometer's stiffness can be precisely adjusted across a wide range, from 3.0×10^{-4} to 2.8×10^{-2} N/m. With this tunable stiffness, the accelerometer achieves remarkable yet flexible sensing performance, including a sensitivity of up to 2068 mm/g and an ultra-broad detection range from ±0.30 mg to ±62.7 mg. These results underscore the feasibility of using tunable stiffness structures to develop diamagnetic levitation accelerometers with flexible sensing capabilities. Experimental validation is undertaken and some of the results obtained could be presented during the conference.

Acknowledgments and conflicts of interest

This work was supported in part by the National Natural Science Foundation of China under Grant 52275537.

Reference

Abadie, J., Piat, E., Oster, S., Boukallel, M., Modeling and experimentation of a passive low frequency nanoforce

sensor based on diamagnetic levitation, Sensors and Actuators A: Physical 173 (2012) 227–237. https://doi.org/10.1016/j.sna.2011.09.025.

Berry, Michael V., and Andre K. Geim. Of flying frogs and levitrons. European Journal of Physics 18.4 (1997): 307. https://doi.org/10.1088/0143-0807/18/4/012

Chen, X., Keşkekler, A., Alijani, F., Steeneken, P.G., Rigid body dynamics of diamagnetically levitating graphite resonators, Applied Physics Letters 116 (2020) 243505. https://doi.org/10.1063/5.0009604.

Chen, X., Kothari, N., Keşkekler, A., Steeneken, P.G., Alijani, F., Diamagnetically levitating resonant weighing scale, Sensors and Actuators A: Physical 330 (2021) 112842. https://doi.org/10.1016/j.sna.2021.112842.

Chen, X., Kothari, N., Keşkekler, A., Steeneken, P.G., Alijani, F., Diamagnetic Composites for High-Q Levitating Resonators, Advanced Science 9 (2022) 2203619. https://doi.org/10.1002/advs.202203619.

Gao, Q.-H., Li, W.-B., Zou, H.-X., Yan, H., Peng, Z.-K., Meng, G., Zhang, W.-M., A centrifugal magnetic levitation approach for high-reliability density measurement, Sensors and Actuators B: Chemical 287 (2019b) 64–70. https://doi.org/10.1016/j.snb.2019.01.150.

Gao, Q., Song, P., Zou, H., Wu, Z., Zhao, L., Zhang, W., Dynamically Rotating Magnetic Levitation to Characterize the Spatial Density Heterogeneity of Materials, Advanced Science 10 (2023) 2300219. https://doi.org/10.1002/advs.202300219.

Gao, Q.-H., Zhang, W.-M, Zou, H.-X., Li, W.-B., Yan, H., Peng, Z.-K., Meng, G., Label-free manipulation via the magneto-Archimedes effect: fundamentals, methodology and applications, Mater. Horiz. 6 (2019a) 1359–1379. https://doi.org/10.1039/C8MH01616J.

Geim, A. K., Simon, M. D., Boamfa, M. I., & Heflinger, L. O. Magnet levitation at your fingertips. Nature, 400(1999), 323-324. https://doi.org/10.1038/22444

Ge, S., Nemiroski, A., Mirica, K.A., Mace, C.R., Hennek, J.W., Kumar, A.A., Whitesides, G.M., Magnetic Levitation in Chemistry, Materials Science, and Biochemistry, Angewandte Chemie International Edition 59 (2020) 17810–17855. https://doi.org/10.1002/anie.201903391.

Hussein, H., Wang, C., Amendoeira Esteves, R., Kraft, M., Fariborzi, H., Near-zero stiffness accelerometer with buckling of tunable electrothermal microbeams, Microsystems & Nanoengineering 10 (2024) 43. https://doi.org/10.1038/s41378-024-00657-w.

Ikezoe, Y., Kaihatsu, T., Sakae, S., Uetake, H., Hirota, N., Kitazawa, K., Separation of feeble magnetic particles with magneto-Archimedes levitation, Energy Conversion and Management 43 (2002) 417–425. https://doi.org/10.1016/S0196-8904(01)00115-7.

Leng, Y., Chen, Y., Li, R., Wang, L., Wang, H., Wang, L., Xie, H., Duan, C.-K., Huang, P., Du, J., Measurement of the Earth Tides with a Diamagnetic-Levitated Micro-Oscillator at Room Temperature, Physical Review Letters 132 (2024) 123601. https://doi.org/10.1103/PhysRevLett.132.123601.

Leng, Y., Li, R., Kong, X., Xie, H., Zheng, D., Yin, P., Xiong, F., Wu, T., Duan, C.-K., Du, Y., Yin, Z., Huang, P., Du, J., Mechanical Dissipation Below 1 μ Hz with a Cryogenic Diamagnetic Levitated Micro-Oscillator, Physical Review Applied 15 (2021) 024061. https://doi.org/10.1103/PhysRevApplied.15.024061.

Middlemiss, R., Bramsiepe, S., Douglas, R., Hough, J., Paul, D., Rowan, S., Hammond, G., Field Tests of a Portable MEMS Gravimeter, Sensors 17 (2017) 2571. https://doi.org/10.3390/s17112571.

Nakashima, R., Diamagnetic levitation of a milligram-scale silica using permanent magnets for the use in a macroscopic quantum measurement, Physics Letters A 384 (2020) 126592. https://doi.org/10.1016/j.physleta.2020.126592.

Pinot, P., Silvestri, Z., New laser power sensor using diamagnetic levitation, Review of Scientific Instruments 88 (2017) 085003. https://doi.org/10.1063/1.4997961.

Qi, W.-H., Yan, G., Lu, J.-J., Liu, F.-R., Zhao, T.-Y., Yan, H., Zhang, W.-M., Local gravity control method for solving load-mismatch issue in isolators, International Journal of Mechanical Sciences 265 (2024) 108891. https://doi.org/10.1016/j.ijmecsci.2023.108891.

Vikrant, K.S., Jayanth, G.R., Diamagnetically levitated nanopositioners with large-range and multiple degrees of freedom, Nature Communications 13 (2022) 3334. https://doi.org/10.1038/s41467-022-31046-4.

Wang, Q., Ren, X., Jiao, S., Lei, X., Zhang, S., Liu, H., Luo, P., Tu, L., A diamagnetic levitation based inertial sensor for geophysical application, Sensors and Actuators A: Physical 312 (2020) 112122. https://doi.org/10.1016/j.sna.2020.112122.

Wang, Y., Xu, Y., Yang, L., Zhou, J., Mahfoud, J., Jin, C., An ultra-sensitive diamagnetic levitation accelerometer with quasi-zero-stiffness structure, Measurement 245 (2025) 116651. https://doi.org/10.1016/j.measurement.2025.116651.

Yin, P., Li, R., Yin, C., Xu, X., Bian, X., Xie, H., Duan, C.-K., Huang, P., He, J., Du, J., Experiments with levitated force sensor challenge theories of dark energy, Nature Physics 18 (2022) 1181–1185. https://doi.org/10.1038/s41567-022-01706-9.

Zhang, K., Su, Y., Ding, J., Gong, Q., Duan, Z., Design and Analysis of a Gas Flowmeter Using Diamagnetic Levitation, IEEE Sensors J. 18 (2018) 6978–6985. https://doi.org/10.1109/JSEN.2018.2853680.